New Physics without bias: Charming Penguins and Lepton Universality Violation in $b \to s\ell^+\ell^-$ decays

Marco Ciuchini,[a] **Marco Fedele,**[b] **Enrico Franco,**[c] **Ayan Paul,**[d,e] **Luca Silvestrini**[c] **and Mauro Valli**[f]

[a]*INFN Sezione di Roma Tre, Via della Vasca Navale 84, I-00146 Rome, Italy*

[b]*Institut für Theoretische Teilchenphysik, Karlsruhe Institute of Technology, D-76131 Karlsruhe, Germany*

[c]*INFN Sezione di Roma, Piazzale Aldo Moro 2, I-00185 Rome, Italy*

[d]*Deutsches Elektronen-Synchrotron DESY, Notkestr. 85, 22607 Hamburg, Germany*

[e]*Institut für Physik, Humboldt-Universität zu Berlin, D-12489 Berlin, Germany*

[f]*C.N. Yang Institute for Theoretical Physics, Stony Brook University, Stony Brook, NY 11794, USA*

E-mail: marco.ciuchini@roma3.infn.it, marco.fedele@kit.edu, enrico.franco@roma1.infn.it, ayan.paul@desy.de, luca.silvestrini@roma1.infn.it, mauro.valli@stonybrook.edu

ABSTRACT: The LHCb experiment has very recently presented new results on Lepton Universality Violation (LUV) in $B \to K^{(*)}\ell^+\ell^-$ decays involving K_S in the final state, which strengthen the recent evidence of LUV obtained in $B^+ \to K^+\ell^+\ell^-$ decays and the previous measurements of $B \to K^{*0}\ell^+\ell^-$. While LUV observables in the Standard Model are theoretically clean, their predictions in New Physics scenarios are sensitive to the details of the hadronic dynamics, and in particular of the charming penguin contribution. In this work, we show how a conservative treatment of hadronic uncertainties is crucial not only to assess the significance of deviations from the Standard Model but also to obtain an unbiased picture of the New Physics responsible for LUV. Adopting a very general parameterization of charming penguins, we find that: *i)* current data hint at a sizable q^2 and helicity dependence of charm loop amplitudes; *ii)* unbiased NP solutions to B anomalies favour a left-handed or an axial lepton coupling rather than a vector one.

1 Introduction

Recently, the LHCb experiment at the Large Hadron Collider has announced evidence of Lepton Universality Violation (LUV) in the ratio [1]

$$R_K[1.1, 6] \equiv \frac{\mathrm{BR}(B^+ \to K^+ \mu^+ \mu^-)}{\mathrm{BR}(B^+ \to K^+ e^+ e^-)}|_{q^2 \in [1.1,6] \mathrm{GeV}^2} = 0.846^{+0.042\,+0.013}_{-0.039\,-0.012}, \qquad (1.1)$$

crowning with success a huge experimental effort aimed at detecting deviations from the Standard Model (SM) in rare B_q decays. Very recently, another piece was added to the already very rich set of data on (semi)leptonic and radiative B_q decays: the measurements of [2]

$$R_{K_S}[1.1, 6] \equiv \frac{\mathrm{BR}(B_d \to K_S \mu^+ \mu^-)}{\mathrm{BR}(B_d \to K_S e^+ e^-)}|_{q^2 \in [1.1,6] \mathrm{GeV}^2} = 0.66^{+0.20\,+0.02}_{-0.14\,-0.04}, \qquad (1.2)$$

$$R_{K^{*+}}[0.045, 6] \equiv \frac{\mathrm{BR}(B^+ \to K^{*+} \mu^+ \mu^-)}{\mathrm{BR}(B^+ \to K^{*+} e^+ e^-)}|_{q^2 \in [0.045,6] \mathrm{GeV}^2} = 0.70^{+0.18\,+0.03}_{-0.13\,-0.04}, \qquad (1.3)$$

complementing the analogous search for LUV in $B \to K^* \ell^+ \ell^-$ decays, R_{K^*} [3, 4], the measurement of $\mathrm{BR}(B_s \to \mu^+ \mu^-)$ [5–9], the angular analyses and BR measurements of $B \to K^{(*)} \mu^+ \mu^-$ [10–12], $B_s \to \phi \mu^+ \mu^-$ [13–16] and $B \to K^* e^+ e^-$ [17, 18]. While hadronic uncertainties make the detection of possible New Physics (NP) contributions to $B_q \to K^{(*)} \ell^+ \ell^-$ differential rates very difficult, at least with current data, any observation of LUV beyond the percent level due to QED corrections [19, 20] would be a clean signal of NP.

In the SM, $b \to s \ell^+ \ell^-$ transitions can only arise at the loop level, as all other Flavour Changing Neutral Current (FCNC) processes, and thus they are particularly sensitive to NP. The leading diagrams giving rise to these transitions are illustrated in Fig. 1. Given the hierarchy in the CKM angles, one has $V_{ub} V_{us}^* \ll V_{cb} V_{cs}^* \sim V_{tb} V_{ts}^*$, making the contribution of virtual up-type quarks in the loops negligible. The GIM mechanism works differently for different diagrams: Z-penguins and boxes vanish as m_q^2 / m_W^2 and are therefore dominated by the top quark, while photonic penguins have a logarithmic dependence on the quark mass, allowing for a large contribution by the charm quark.

Another fundamental difference between the two classes of diagrams is due to the chirality of the weak couplings: Z-penguins and boxes involve both vector and axial couplings to leptons, while photon penguins couple vectorially to leptons. This implies that the top-dominated Z-penguins and boxes give rise to the local operators $Q_{9V} \sim \bar{b} \gamma^\mu P_L s \bar{\ell} \gamma_\mu \ell$ and $Q_{10A} \sim \bar{b} \gamma^\mu P_L s \bar{\ell} \gamma_\mu \gamma_5 \ell$ at the electroweak scale. Photonic penguins instead are more complicated: the top quark contributes to Q_{9V} at the electroweak scale, but the charm quark remains dynamic at the scale m_b and therefore contributes to $b \to s \ell^+ \ell^-$ transitions both via the local operator Q_{9V} and via the (potentially nonlocal and nonperturbative) matrix elements of current-current operators involving the charm quark, $Q_{1,2}^{\bar{b} c \bar{c} s} \sim \bar{b} \gamma^\mu P_L c \bar{c} \gamma_\mu P_L s$, denoted by charming penguins [21–23]. This complication, however, does not affect axial lepton couplings, which remain purely short-distance.

Computing the matrix element of $Q_{1,2}^{\bar{b} c \bar{c} s}$ is a formidable task. While the calculation of decay amplitudes for exclusive $b \to s \ell^+ \ell^-$ transitions is well-defined in the infinite b
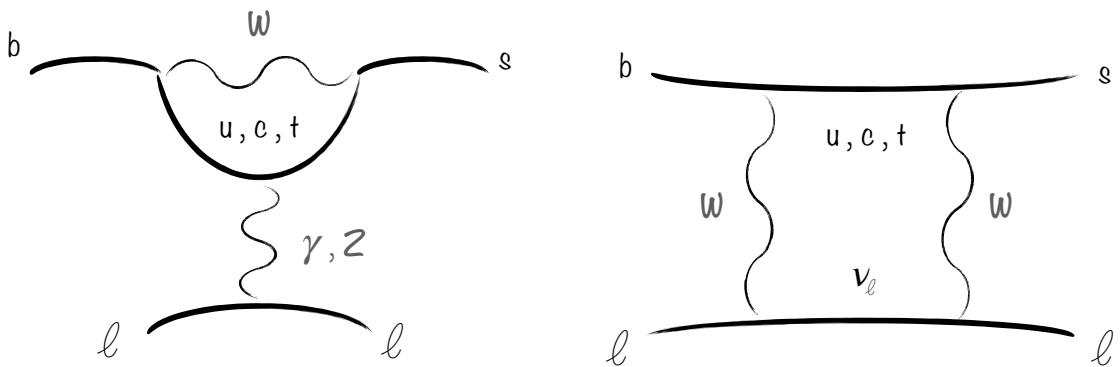
Figure 1. Penguin and box diagrams giving rise to $b \to s\ell^+\ell^-$ transitions in the SM.

and c mass limit [24–26], and while in the same limit the uncertainty from decay form factors can be eliminated by taking suitable ratios of observables [27, 28], in the real world amplitude calculations must cope with power corrections [29, 30], which can be sizable or even dominant in several kinematic regions [31–35]. For example, the Operator Product Expansion is known to fail altogether for resonant $B \to K^{(*)}J/\psi \to K^{(*)}\mu^+\mu^-$ transitions [36], and its accuracy is questionable close to the $c\bar{c}$ threshold. For this reason, estimating corrections to QCD factorization in the low dilepton invariant mass (low-q^2) region of $B \to K^{(*)}\ell^+\ell^-$ and $B_s \to \phi\ell^+\ell^-$ decay amplitudes is a crucial step towards a reliable assessment of possible deviations from SM predictions in these decay channels. Unfortunately, first-principle calculations of these power corrections are not currently available, and a theoretical breakthrough would be needed to perform such calculations, see, e.g., the discussion in [30, 37, 38].

Therefore, as of now, a conservative analysis of semileptonic B decays can only rely on the use of data-driven methods to account for the theoretical uncertainties and to quantify possible deviations from the SM. In this regard, it is important to stress that while the contribution of Q_{9V} to the decay amplitude should depend on helicity and on q^2 according to the form factors, long-distance contributions from the charm loop matrix element should show some additional helicity and q^2 dependence. It is then very interesting to use a q^2 and helicity-dependent parameterization of power corrections [29, 30] when analyzing experimental data: A sizable deviation from what expected from purely local matrix elements would be a clear confirmation of the presence of power corrections.

Obviously, the charm loop matrix element cannot generate any Lepton Universality Violation (LUV), so that ratios of decay Branching Ratios (BRs) for different leptons in the final state can be very reliably predicted in the SM [19, 20, 39, 40]. However, once lepton non-universal NP is introduced, the hadronic uncertainty related to the charm loop creeps back in, due to the interference between SM and NP contributions in decay amplitudes, so that the inference of NP parameters from LUV observables is not free from hadronic uncertainties. Thus, the relevance of a careful and conservative treatment of hadronic uncertainties in assessing the compatibility of $b \to s\ell^+\ell^-$ data with the SM, and in inferring what kind of NP could lie behind the evidence of LUV, cannot be overstated.

Several analyses [41–46] have recently discussed the implications for NP of the so-called "clean" observables: LUV measurements and $\mathrm{BR}(B_s \to \mu^+\mu^-)$, albeit without particular focus on the impact that hadronic uncertainties can have in the determination of the emerging NP picture. The aforementioned "clean" observables have also been considered together with other interesting tensions with the SM, see for instance [47–49] for the case of the so-called "Cabibbo anomaly", and refs. [50–57] for possible connections with the long-standing puzzle of the magnetic dipole moment of the muon.

In this work, we focus on $b \to s\ell^+\ell^-$ transitions in a bottom-up perspective. Building on our previous analyses [31, 32, 34, 58–60] and on the data presented in [1–18], we aim at answering two fundamental, and deeply related, questions:

1. Do current data on differential BRs display a non-trivial q^2 and helicity dependence of charming penguins, pointing to sizable long-distance effects?

2. What is the overall significance for NP in light of the new data, and how do hadronic uncertainties affect the interpretation of the present evidence of LUV?

To this end, following the strategy we originally proposed in ref. [31], in the following we consider a generic parameterization for non-factorizable QCD power corrections without theoretical bias, and let data determine the q^2 and helicity dependence of charming penguins. In this way, we achieve a fully unbiased inference on NP contributions.

Notice that the approach recently followed in ref. [61] to allow for an arbitrary lepton-universal correction ΔC_9^U to C_9 is less general, and therefore less conservative, than our approach, unless ΔC_9^U is promoted from a parameter to a q^2- and helicity-dependent function.

The paper is organized as follows: in section 2 we present our parameterization for charming penguins and discuss the implications of current data on QCD long-distance effects; in section 3 we present an unbiased global analysis of NP effects using both the Standard Model Effective Field Theory (SMEFT) and the Weak Effective Hamiltonian; in section 4 we wrap up the present study with our conclusions.

2   Charming penguins from current data

For the convenience of the reader, let us briefly summarize our approach to hadronic uncertainties. We write down the helicity-dependent SM decay amplitudes for $B \to K^*\ell^+\ell^-$ in the following way [29, 62]:

$$H_V^\lambda \propto \left\{ C_9^{\mathrm{SM}}\widetilde{V}_{L\lambda} + \frac{m_B^2}{q^2}\left[\frac{2m_b}{m_B}C_7^{\mathrm{SM}}\widetilde{T}_{L\lambda} - 16\pi^2 h_\lambda\right]\right\},$$

$$H_A^\lambda \propto C_{10}^{\mathrm{SM}}\widetilde{V}_{L\lambda}\,, \;\; H_P \propto \frac{m_\ell\, m_b}{q^2}\, C_{10}^{\mathrm{SM}}\left(\widetilde{S}_L - \frac{m_s}{m_b}\widetilde{S}_R\right) \tag{2.1}$$

with $\lambda = 0, \pm$ and $C_{7,9,10}^{\mathrm{SM}}$ the SM Wilson coefficients of the operators Q_{9V}, Q_{10A} and $Q_{7\gamma} \sim m_b\bar{b}_R\sigma_{\mu\nu}F^{\mu\nu}s_L$ normalized as in ref. [59].

The factorizable part of the amplitudes corresponds to seven independent form factors, $\widetilde{V}_{0,\pm}$, $\widetilde{T}_{0,\pm}$ and $\widetilde{S}$, smooth functions of q^2 [63, 64]. Instead, $h_\lambda(q^2)$ represents the

non-factorizable part of the amplitude [30, 31, 65], dominated by the charming penguin contribution. Nonperturbative methods working in Euclidean spacetime such as lattice QCD cannot directly evaluate $h_\lambda(q^2)$ as at present there is no way to evade the Maiani-Testa no-go theorem [66], which prevents the computation of rescattering and final state interactions away from the threshold. Light-cone sum rules can be used to obtain a model-dependent estimate of the charming penguin for $q^2 \ll m_c^2$ [67, 68]; however, the problem of extrapolating to larger values of q^2 remains challenging, given the complicated analytic structure of the decay amplitude. For example, long-distance effects such as rescattering from $D_s^{(*)} - \bar{D}^{(*)}$ intermediate states do not correspond to a cut in q^2 and therefore are difficult to account for in the context of a q^2 interpolation.

Given our ignorance of the charming penguin amplitude, we parameterize the hadronic contribution as follows [34]:

$$H_V^- \propto \frac{m_B^2}{q^2} \left[\frac{2m_b}{m_B} \left(C_7^{\mathrm{SM}} + h_-^{(0)} \right) \widetilde{T}_{L-} - 16\pi^2 h_-^{(2)} q^4 \right] + \left(C_9^{\mathrm{SM}} + h_-^{(1)} \right) \widetilde{V}_{L-} \,,$$

$$H_V^+ \propto \frac{m_B^2}{q^2} \left[\frac{2m_b}{m_B} \left(C_7^{\mathrm{SM}} + h_-^{(0)} \right) \widetilde{T}_{L+} - 16\pi^2 \left(h_+^{(0)} + h_+^{(1)} q^2 + h_+^{(2)} q^4 \right) \right] + \left(C_9^{\mathrm{SM}} + h_-^{(1)} \right) \widetilde{V}_{L+} \,,$$

$$H_V^0 \propto \frac{m_B^2}{q^2} \left[\frac{2m_b}{m_B} \left(C_7^{\mathrm{SM}} + h_-^{(0)} \right) \widetilde{T}_{L0} - 16\pi^2 \sqrt{q^2} \left(h_0^{(0)} + h_0^{(1)} q^2 \right) \right] + \left(C_9^{\mathrm{SM}} + h_-^{(1)} \right) \widetilde{V}_{L0} \,. \quad (2.2)$$

In the expressions above it is evident that $h_-^{(0)}$ is equivalent to a shift in C_7, i.e. ΔC_7, while $h_-^{(1)}$ corresponds to a lepton universal correction ΔC_9. On the other hand, the remaining h parameters appearing in (2.2) are not equivalent to a shift in the Wilson coefficients of $Q_{7\gamma, 9V}$ and thus they represent genuine hadronic effects.

As discussed in detail in [31, 67], the hadronic contributions introduced above correspond to the following q^2- and helicity-dependent shifts in C_9:

$$\Delta C_{9,1}(q^2) = -\frac{16 m_B^3 (m_B + m_{K^*}) \pi^2}{\sqrt{\lambda(q^2)} V(q^2) q^2} (h_-(q^2) - h_+(q^2))$$

$$\Delta C_{9,2}(q^2) = -\frac{16 m_B^3 \pi^2}{(m_B + m_{K^*}) A_1(q^2) q^2} (h_-(q^2) + h_+(q^2))$$

$$\Delta C_{9,3}(q^2) = -\frac{16 m_B^3 (m_B + m_{K^*})(m_B^2 - q^2 - m_{K^*}^2) \pi^2}{\lambda(q^2) A_2(q^2) q^2} (h_-(q^2) + h_+(q^2))$$

$$+ \frac{64 \pi^2 m_B^3 m_{K^*} \sqrt{q^2} (m_B + m_{K^*})}{\lambda(q^2) A_2(q^2) q^2} h_0(q^2) \,. \quad (2.3)$$

An analogous parameterization can be introduced for charming penguins in $B \to K \ell^+ \ell^-$, as well as for $B_s \to \phi \ell^+ \ell^-$. When considering hadronic contributions in $B \to K^*$ decays versus those in $B_s \to \phi$ decays the consideration of flavour SU(3) breaking comes into play. Given that the degree of SU(3) breaking originating from $m_s \gg m_d, m_u$ is not quantifiable ab initio, we performed some tests by adding ad hoc SU(3) breaking parameters that multiplicatively modifies the hadronic terms in $B_s \to \phi$ decays vis-à-vis those in $B \to K^*$ decays, i.e.,

$$h_\lambda^{B_s \to \phi} = (1 + \delta_R + i\delta_I) h_\lambda^{B \to K^*} \,. \quad (2.4)$$
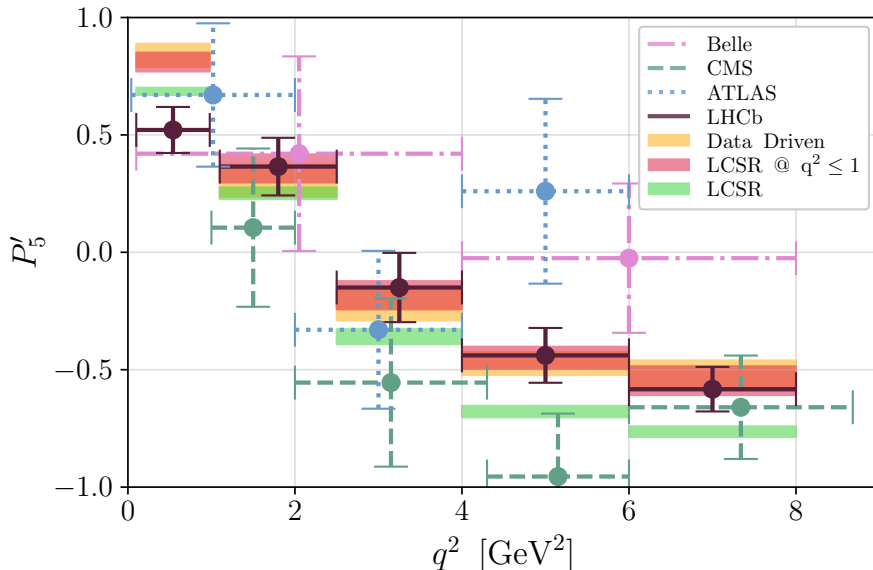
Figure 2. The result for the optimized observable P_5' (see ref. [69]) from a global fit within the SM in three different approaches for the charming penguin contribution, compared to experimental data. Only the approach fully relying on LCSR estimates (refs. [67, 68]) in the entire dilepton invariant-mass range may lead to the so-called "P_5' anomaly". See text for more details.

The two parameters, δ_R and δ_I, are taken for simplicity to be independent of helicity and simply modify the real and imaginary parts of the hadronic terms independently. We set a Gaussian prior on δ_R and δ_I with $\mu = 0$ and $\sigma = 0.3$ representative of 30% SU(3) breaking centered at no SU(3) breaking. The posterior distribution of δ_R and δ_I are not significantly different from the prior distributions leading us to conclude that the experimental results are not precise enough to draw conclusion about $SU(3)$ breaking within this hypothesis. For the rest of the discussion we assume exact flavour $SU(3)$ symmetry for power corrections, which is justified given the current experimental uncertainties. In the future, realistic departures from the $SU(3)$ limit could be probed by data and the present investigation of QCD effects could be further generalized along these lines in a straightforward manner.

Using the `HEPfit` code [70, 71] and the form factors and input parameters used in Refs. [31, 32, 34, 58–60], we perform a Bayesian fit to the data in refs. [5–18] within the SM, adopting three distinct approaches to account for power corrections to factorization:

1. A *fully model-dependent* approach in which LCSR results are extrapolated over the full range of q^2 [37, 67, 68, 72, 73] – labeled in our figures as "LCSR". Within this approach, the size of charming penguins in $B \to K^* \ell^+ \ell^-$ is comparable to the ones provided by factorizable QCD power corrections, while the size of charming penguins in $B \to K \ell^+ \ell^-$ is too small to be phenomenologically relevant.

2. A *partly model-dependent* approach in which LCSR results are used only for $q^2 \leq 1$ GeV^2 – denoted in figures as "LCSR @ $q^2 \leq 1$". Within this approach, the size of charming penguins in $B \to K^* \ell^+ \ell^-$ can depart from the LCSR estimate once away
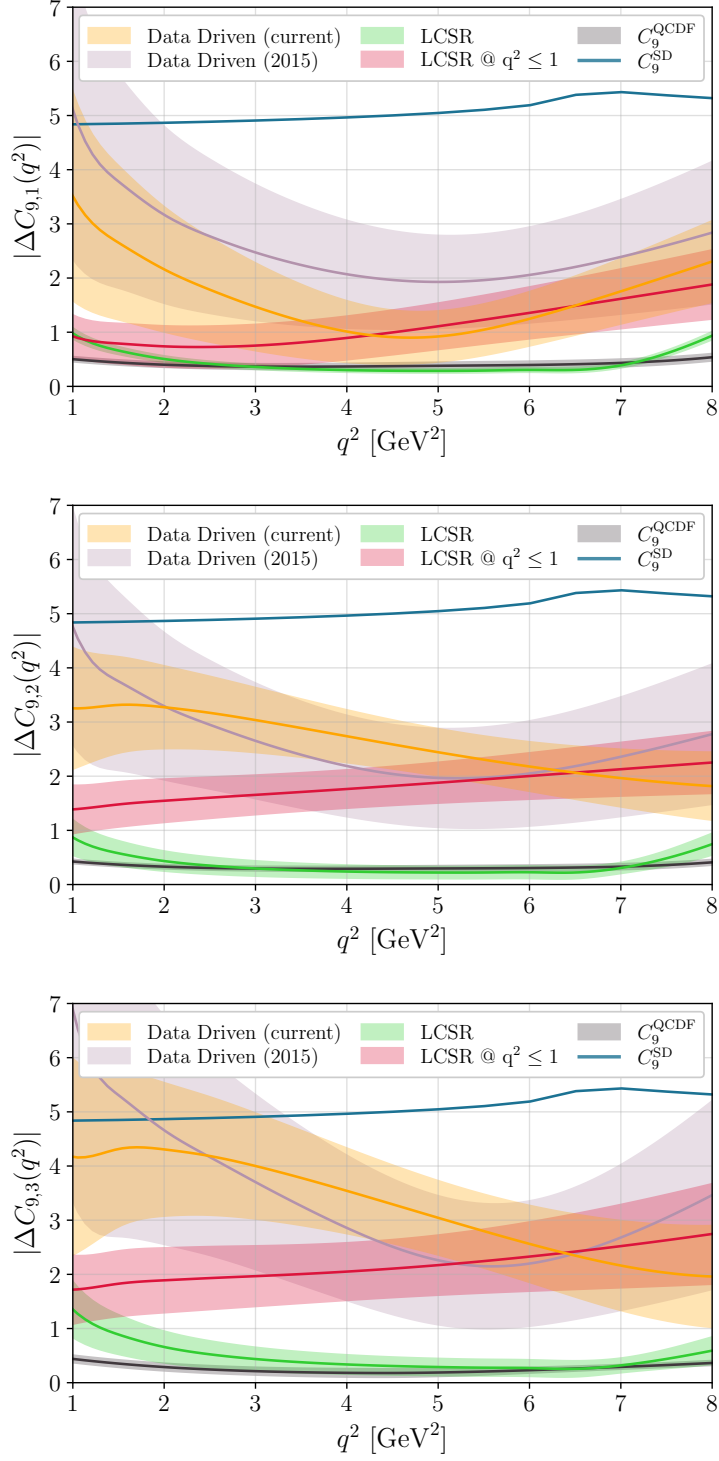
Figure 3. 95% probability contours of the posteriors for the functions $\Delta C_{9,i}(q^2)$ defined in eq. (2.3) in the three approaches for charming penguins. For comparison, the result obtained in the data-driven approach with 2015 data is also reported, along with the short-distance contribution and the factorizable QCD corrections.

from the light-cone region, while charm-loop effects in $B \to K\ell^+\ell^-$ are still regarded as negligible in light of the estimates in refs. [67, 68].

3. A *fully data driven* approach in which all h parameters are determined from experimental data – labeled by "Data Driven". Here, the size of power corrections can be comparable to the perturbative contributions for all decay channels.

In Fig. 2, as a representative example, we show the outcome of the fit in the SM for the optimized observable P_5' [69] in the three different approaches to power corrections. As shown in the plot, no tension from data emerges from this observable in the Data Driven approach or in the partly model-dependent one. In general, as already noted in [31], an excellent fit to the data (except, of course, for LUV ratios and with the notable other exception of the time-integrated $\mathrm{BR}(B_s \to \mu^+\mu^-)$) can be obtained within these two approaches. On the other hand, LCSR results extrapolated to larger values of q^2 yield a poor fit of several BRs as well as tension in some of the angular observables, giving rise to the so-called P_5' anomaly.

The result shown for P_5' highlights the major role played by long-distance effects. In Fig. 3, we further investigate this aspect showing the q^2 and helicity dependence of the charming penguin contributions. In the plot we show the 95% probability regions of the posteriors for the functions $\Delta C_{9,i}(q^2)$ obtained in the global fit in the SM under the three different approaches. In the same figure, as a guideline, we also show the size of the SM short-distance contribution to Q_{9V}, labeled by C_9^{SD}, as well as the size of the factorizable QCD corrections.

The posteriors of $\Delta C_{9,i}(q^2)$ in Fig. 3 display non-negligible hadronic contributions – comparable in size to C_9^{SD} rather than C_9^{QCDF} – in the whole region of low dilepton mass probed by current data. This is not surprising since power corrections are naively expected to be larger than perturbative QCD corrections of $\mathcal{O}(\alpha_s/(4\pi))$ [21–23]. A departure from LCSR expectations even at very low q^2 is hinted at in the Data Driven approach, which matches the outcome of the partly model-dependent one only for $q^2 \gtrsim 4m_c^2$.

As can also be seen in Fig. 3, by comparing the Data Driven determination of $\Delta C_{9,i}(q^2)$ from current data with the one obtained in our 2015 analysis [31][1] it is evident how improved data on differential BR's allow for a much better knowledge of the charm contribution. In this respect, it will be interesting to see whether more precise data will bring stronger evidence of such hadronic effects. At present, hints of large hadronic contributions from data are still statistically mild, as can be read from Table 1. There, we report the highest probability density intervals (HPDI) for the posteriors of the h parameters adopted in the two more conservative approaches. Some h's corresponding to genuine hadronic contributions deviate from 0, but still only at the 2σ level.

In conclusion, the *fully data driven* scenario stands out as the most conservative choice for an unbiased inference on NP contributions. In the following we take it as a reference, but for completeness we present results on NP also in the other two approaches.

---

[1]The outcome of the 2015 analysis has been rederived adopting the h's parameterization of this work.

Hadronic parameter	Approach	68% HPDI	95% HPDI
$\operatorname{Re} h_0^{(0)} \times 10^4$	Data Driven	$[1.69, 5.83]$	$[-0.26, 8.33]$
	LCSR $q^2 \leq 1$	$[1.91, 5.25]$	$[0.26, 7.12]$
$\operatorname{Im} h_0^{(0)} \times 10^4$	Data Driven	$[-4.56, 2.76]$	$[-8.44, 6.52]$
	LCSR $q^2 \leq 1$	$[-4.30, 0.21]$	$[-6.21, 2.84]$
$\operatorname{Re} h_+^{(0)} \times 10^4$	Data Driven	$[-1.25, -0.34]$	$[-1.73, 0.12]$
	LCSR $q^2 \leq 1$	$[-0.18, 0.07]$	$[-0.34, 0.19]$
$\operatorname{Im} h_+^{(0)} \times 10^4$	Data Driven	$[-0.40, 0.65]$	$[-0.92, 1.22]$
	LCSR $q^2 \leq 1$	$[-0.12, 0.11]$	$[-0.26, 0.25]$
$\operatorname{Re} h_-^{(0)} \equiv \operatorname{Re} \Delta C_7 \times 10^2$	Data Driven	$[-0.30, 2.98]$	$[-2.08, 4.85]$
	LCSR $q^2 \leq 1$	$[-1.06, 1.41]$	$[-2.12, 2.37]$
$\operatorname{Im} h_-^{(0)} \equiv \operatorname{Im} \Delta C_7 \times 10^2$	Data Driven	$[-8.89, 1.39]$	$[-14.15, 6.57]$
	LCSR $q^2 \leq 1$	$[-3.27, -0.66] \cup [1.46, 1.60]$	$[-3.64, 2.75]$
$\operatorname{Re} h_0^{(1)} \times 10^5$	Data Driven	$[-3.61, 1.88]$	$[-6.52, 5.09]$
	LCSR $q^2 \leq 1$	$[-1.87, 3.03]$	$[-4.26, 5.95]$
$\operatorname{Im} h_0^{(1)} \times 10^5$	Data Driven	$[-7.59, 2.26]$	$[-11.41, 7.67]$
	LCSR $q^2 \leq 1$	$[-5.04, 3.82]$	$[-8.81, 8.38]$
$\operatorname{Re} h_+^{(1)} \times 10^4$	Data Driven	$[1.33, 2.78]$	$[0.52, 3.51]$
	LCSR $q^2 \leq 1$	$[0.10, 0.90]$	$[-0.33, 1.29]$
$\operatorname{Im} h_+^{(1)} \times 10^4$	Data Driven	$[0.77, 2.64]$	$[-0.32, 3.48]$
	LCSR $q^2 \leq 1$	$[0.03, 0.89]$	$[-0.45, 1.29]$
$\operatorname{Re} h_-^{(1)} \equiv \operatorname{Re} \Delta C_9$	Data Driven	$[-0.02, 1.23]$	$[-0.68, 1.87]$
	LCSR $q^2 \leq 1$	$[-0.32, 0.73]$	$[-0.88, 1.23]$
$\operatorname{Im} h_-^{(1)} \equiv \operatorname{Im} \Delta C_9$	Data Driven	$[-0.90, 2.68]$	$[-2.69, 4.58]$
	LCSR $q^2 \leq 1$	$[-0.05, 1.91]$	$[-1.40, 2.47]$
$\operatorname{Re} h_+^{(2)} \times 10^5$	Data Driven	$[-3.61, -1.09]$	$[-4.93, 0.23]$
	LCSR $q^2 \leq 1$	$[-0.99, 0.71]$	$[-1.83, 1.63]$
$\operatorname{Im} h_+^{(2)} \times 10^5$	Data Driven	$[-4.25, -1.14]$	$[-5.74, 0.59]$
	LCSR $q^2 \leq 1$	$[-1.71, 0.22]$	$[-2.63, 1.23]$
$\operatorname{Re} h_-^{(2)} \times 10^5$	Data Driven	$[0.15, 1.77]$	$[-0.70, 2.65]$
	LCSR $q^2 \leq 1$	$[0.98, 2.33]$	$[0.29, 3.05]$
$\operatorname{Im} h_-^{(2)} \times 10^5$	Data Driven	$[-1.96, 2.10]$	$[-4.11, 4.15]$
	LCSR $q^2 \leq 1$	$[-1.40, 1.30]$	$[-2.61, 2.79]$

Table 1. 68% and 95% HPDI of the posterior distribution of the hadronic parameters $h_\lambda^{(i)}$. The red color highlights ranges not including 0. Genuine hadronic effects encoded in $h_0^{(0)}$ and $h_-^{(2)}$ are found to be non-vanishing at the 2σ level in the partly model-dependent approach, while $h_+^{(1)}$ deviates from zero at more than 2σ in the Data Driven fit.

3 New Physics in B decays without bias

While experimental data on BR's and angular distributions can be reproduced within the SM in both the *fully data driven* and in the *partly model-dependent* scenarios, reproducing the central values of the LUV ratios for $B \to K^{(*)}\ell^+\ell^-$, as well as the current measurement of $\mathrm{BR}(B_s \to \mu^+\mu^-)$, undoubtedly requires physics beyond the SM.

Given the bounds from direct searches of NP at the LHC, it is reasonable to assume in this context that NP contributions would arise at energies much larger than the weak scale. Then, a suitable framework to describe such contributions is given by the SMEFT, in particular by adding to the SM the following additional dimension-six operators:[2]

$$
\begin{aligned}
O_{2223}^{LQ^{(1)}} &= (\bar{L}_2\gamma_\mu L_2)(\bar{Q}_2\gamma^\mu Q_3)\,, \\
O_{2223}^{LQ^{(3)}} &= (\bar{L}_2\gamma_\mu \tau^A L_2)(\bar{Q}_2\gamma^\mu \tau^A Q_3)\,, \\
O_{2322}^{Qe} &= (\bar{Q}_2\gamma_\mu Q_3)(\bar{e}_2\gamma^\mu e_2)\,, \\
O_{2223}^{Ld} &= (\bar{L}_2\gamma_\mu L_2)(\bar{d}_2\gamma^\mu d_3)\,, \\
O_{2223}^{ed} &= (\bar{e}_2\gamma_\mu e_2)(\bar{d}_2\gamma^\mu d_3)\,,
\end{aligned}
\tag{3.1}
$$

where $\tau^{A=1,2,3}$ are Pauli matrices (a sum over A in the equations above is understood), weak doublets are in upper case and $SU(2)_L$ singlets are in lower case, and flavour indices are defined in the basis of diagonal down-type quark Yukawa couplings. Since in our analysis operators $O_{2223}^{LQ^{(1,3)}}$ always enter as a sum, we collectively denote their Wilson coefficient as C_{2223}^{LQ}. For concreteness, we normalize SMEFT Wilson coefficients to a NP scale $\Lambda_{\mathrm{NP}} = 30$ TeV and we only consider NP contributions to muons.[3] Matching the SMEFT operators onto the weak effective Hamiltonian one obtains the following contributions to operators Q_{9V} and Q_{10A} and to the chirality-flipped Q'_{9V} and Q'_{10A} [78]:

$$
\begin{aligned}
C_9^{\mathrm{NP}} &= \frac{\pi v^2}{\alpha_e \lambda_t \Lambda_{\mathrm{NP}}^2}\left(C_{2223}^{LQ^{(1)}} + C_{2223}^{LQ^{(3)}} + C_{2322}^{Qe}\right)\,, \\
C_{10}^{\mathrm{NP}} &= \frac{\pi v^2}{\alpha_e \lambda_t \Lambda_{\mathrm{NP}}^2}\left(C_{2322}^{Qe} - C_{2223}^{LQ^{(1)}} - C_{2223}^{LQ^{(3)}}\right)\,, \\
C_9^{\prime,\mathrm{NP}} &= \frac{\pi v^2}{\alpha_e \lambda_t \Lambda_{\mathrm{NP}}^2}\left(C_{2223}^{ed} + C_{2223}^{Ld}\right)\,, \\
C_{10}^{\prime,\mathrm{NP}} &= \frac{\pi v^2}{\alpha_e \lambda_t \Lambda_{\mathrm{NP}}^2}\left(C_{2223}^{ed} - C_{2223}^{Ld}\right)\,,
\end{aligned}
\tag{3.2}
$$

with α_e the fine-structure constant, v the vacuum expectation value of the SM Higgs field, $\lambda_t = V_{ts}V_{tb}^*$, and alignment in the down-quark sector assumed, i.e. $Q_i = (V_{ji}^* u_{jL}, d_{jL})^T$ [59].

We perform a Bayesian fit to the data in refs. [1–18] in several NP scenarios characterized by different combinations of nonvanishing Wilson coefficients. To perform model

---

[2]Notice that these operators may be further generated at one loop via SM RGE effects, see, e.g., refs. [74, 75]. In addition, here we do not consider the possibility that, integrating out NP, one would generate sizable $Q_{1,2}^{b\bar{c}\bar{c}s}$ as studied e.g. in [76, 77].

[3]The focus on LUV effects in muons is mainly motivated by the $\sim 2.3\sigma$ tension of the SM with the current experimental average for the time-integrated $\mathrm{BR}(B_s \to \mu^+\mu^-)$.

NP scenario	Approach	68% HPDI	ΔIC
A: C_9^{NP}	Data Driven	$[-3.04, -1.10] \cup [1.48, 1.99]$	$21 \cup 13$
	LCSR $q^2 \leq 1$	$[-1.44, -1.01]$	43
	LCSR	$[-1.37, -1.12]$	94
B: C_{2223}^{LQ}	Data Driven	$[0.65, 1.05]$	38
	LCSR $q^2 \leq 1$	$[0.67, 0.88]$	60
	LCSR	$[0.77, 0.96]$	75
C: C_{10}^{NP}	Data Driven	$[0.53, 0.79]$	39
	LCSR $q^2 \leq 1$	$[0.66, 0.90]$	54
	LCSR	$[0.56, 0.79]$	20
D: $\{C_{2223}^{LQ}, C_{2322}^{Qe}\}$	Data Driven	$\{[0.20, 1.03], [-0.82, 0.15]\}$	37
	LCSR $q^2 \leq 1$	$\{[0.61, 0.86], [-0.37, 0.11]\}$	57
	LCSR	$\{[0.90, 1.10], [0.53, 0.79]\}$	96
D: $\{C_9^{\mathrm{NP}}, C_{10}^{\mathrm{NP}}\}$	Data Driven	$\{[-0.81, 0.46], [0.51, 0.83]\}$	37
	LCSR $q^2 \leq 1$	$\{[-0.67, -0.20], [0.47, 0.76]\}$	57
	LCSR	$\{[-1.33, -1.06], [0.15, 0.34]\}$	96
E: $\{C_{2223}^{LQ}, C_{2322}^{Qe}, C_{2223}^{Ld}, C_{2223}^{ed}\}$	Data Driven	$\{[-0.06, 1.18], [-0.99, 0.35], [-1.30, 0.34], [-1.25, 0.56]\}$	30
	LCSR $q^2 \leq 1$	$\{[0.83, 1.32], [-0.05, 0.76], [-0.59, -0.10], [-0.58, 0.27]\}$	54
	LCSR	$\{[1.03, 1.23], [0.69, 0.97], [-0.49, -0.17], [-0.25, 0.43]\}$	105
E: $\{C_9^{\mathrm{NP}}, C_{10}^{\mathrm{NP}}, C_9'^{,\mathrm{NP}}, C_{10}'^{,\mathrm{NP}}\}$	Data Driven	$\{[-1.05, 0.75], [0.38, 0.81], [-0.57, 1.82], [-0.31, 0.12]\}$	30
	LCSR $q^2 \leq 1$	$\{[-1.45, -0.59], [0.29, 0.70], [-0.06, 0.82], [-0.37, 0.08]\}$	54
	LCSR	$\{[-1.55, -1.27], [0.11, 0.31], [-0.17, 0.52], [-0.47, -0.14]\}$	105

Table 2. 68% HPDI of the posterior distribution of the SMEFT Wilson coefficients from a fit to the full set of $b \to s\ell^+\ell^-$ data in the NP scenarios A, B, C, D and E, along with $\Delta IC \equiv IC_{\mathrm{SM}} - IC_{\mathrm{NP}}$.

comparison of different scenarios, we compute the *Information Criterion* (IC) [79]:

$$IC \equiv -2\overline{\log \mathcal{L}} + 4\sigma_{\log \mathcal{L}}^2 , \qquad (3.3)$$
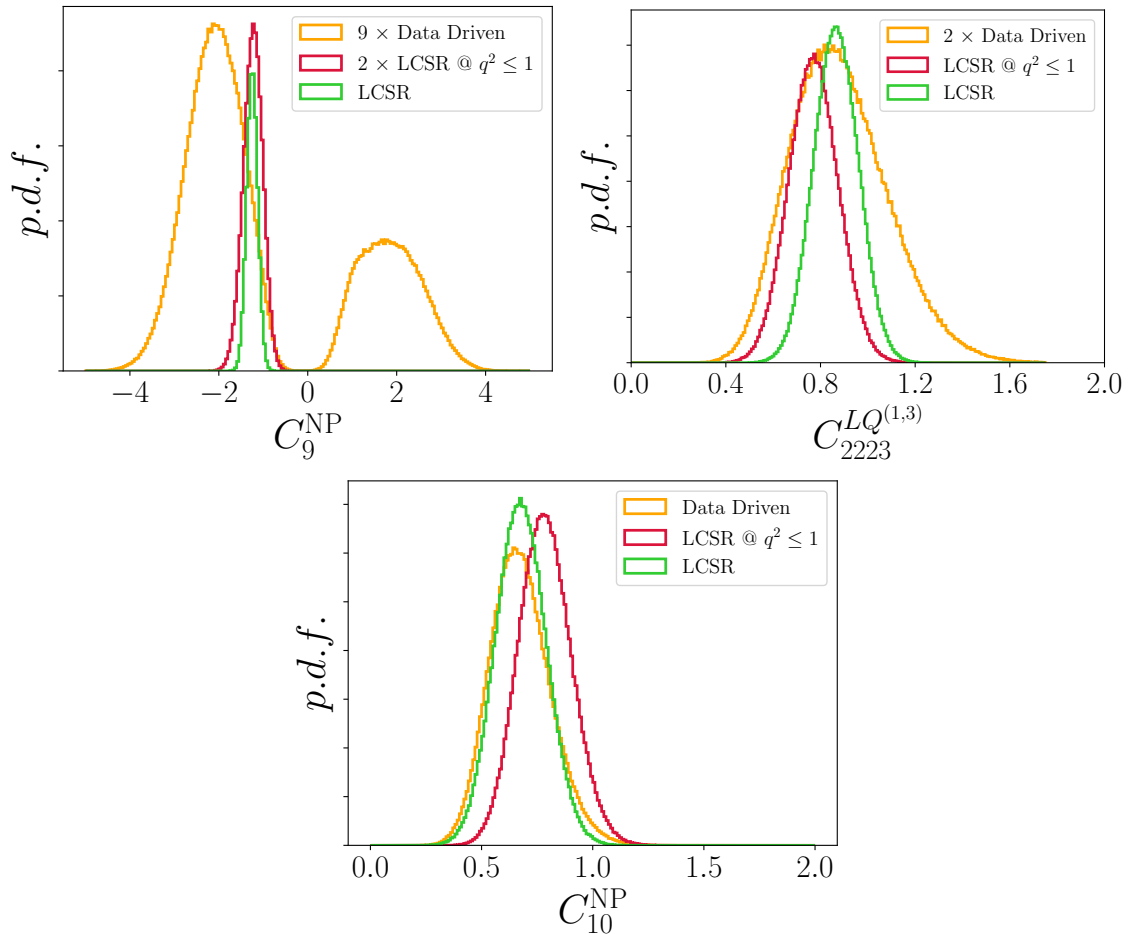
Figure 4. Probability density function (p.d.f.) for $C_9^{\rm NP}$ (first panel), C_{2223}^{LQ} (second panel) and $C_{10}^{\rm NP}$ (third panel). Green, red and orange p.d.f.'s correspond to *fully model-dependent*, *partly model-dependent* and *fully data driven* approaches respectively.

where the first and second terms represent mean and variance of the log likelihood posterior distribution, respectively. The first term measures the quality of the fit, while the second one counts effective degrees of freedom and thus penalizes more complicated models. Models with smaller IC should be preferred according to the canonical scale of evidence of Ref. [80], related in this context to (positive) IC differences. For convenience, we always report $\Delta IC \equiv IC_{\rm SM} - IC_{\rm NP}$.

As is evident from the discussion in section 2, different assumptions on charming penguins yield different results on NP Wilson coefficients, since LUV ratios depend on the charm loop through the interference between NP and SM contributions. It goes without saying that a conservative inference on NP requires a conservative, *i.e. fully data driven*, estimate of charming penguins. Of course, since the SM reproduces much better experimental data in the *fully data driven* and *partly model-dependent* approaches than in the *fully model-dependent* one, with the first scenario performing better than the second one, NP ΔIC's (or equivalently the significance of NP) will be smallest in the *fully data driven*
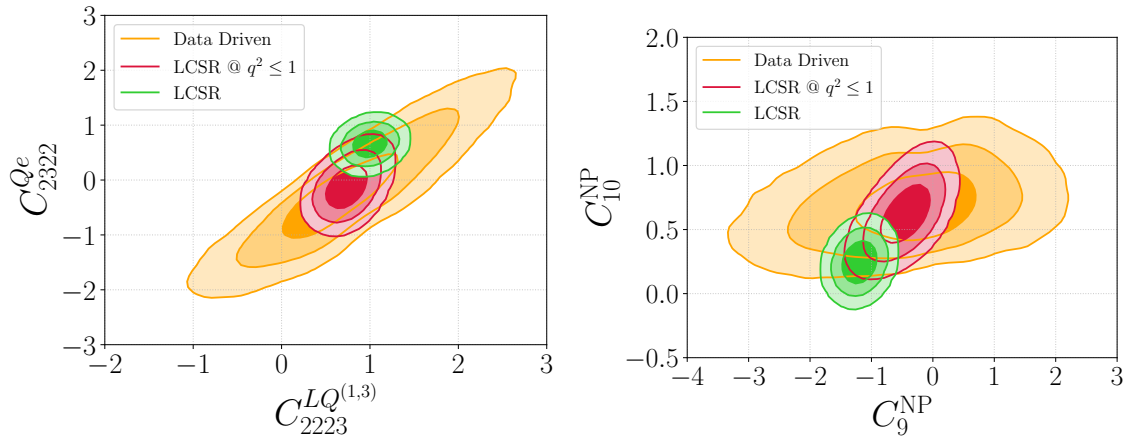
Figure 5. Posteriors in the $(C_{2223}^{LQ}, C_{2322}^{Qe})$ plane (first panel) and in the (C_9^{NP}, C_{10}^{NP}) plane (second panel). The colour scheme is defined in the caption of Fig. 4. Contours correspond to smallest regions of 68.3%, 95.4% and 99.7% probability.

approach and largest in the *fully model-dependent* one.

Let us first consider three very simple NP scenarios: scenario A, in which deviations can only arise in C_9, scenario B, in which only C_{2223}^{LQ} can be nonvanishing, corresponding to $C_9^{NP} = -C_{10}^{NP}$, and scenario C, in which only C_{10}^{NP} is allowed to float. Already in these simple NP scenarios there are dramatic differences in the fit depending on the assumption on charming penguins. Under the *fully data driven* and *partly model-dependent* assumptions, scenarios B and C perform much better than scenario A, while the opposite is true in the *fully model-dependent* case. As reported in the left panel of Fig. 4, in the *fully data driven* approach charming penguins can even interfere destructively with C_9^{NP}, allowing for a second solution for LUV observables with positive C_9^{NP}, albeit with a smaller ΔIC with respect to the solution with negative C_9^{NP} (see Table 2). In the *fully model-dependent* case, scenario A is ideal since it allows to strongly improve the agreement of both LUV and angular observables, while in scenario B the constraint from $B_s \rightarrow \mu^+\mu^-$ limits the improvement in angular observables (see Table 3), and scenario C cannot improve the agreement with angular observables at all. Conversely, under the *fully data driven* hypothesis, scenarios B and C allow to reproduce all observables, including LUV and $B_s \rightarrow \mu^+\mu^-$, with a minimal set of NP coefficients, and therefore stand out as the preferred NP scenarios. The *partly model-dependent* case is in a somewhat intermediate position, with scenario C somewhat disfavoured with respect to scenario B due to the constraints on the charming penguin at low q^2. Obviously, as can be seen in Fig. 4, the p.d.f. for C_{10}^{NP} in scenario C is almost independent of the hadronic uncertainties, while the overall quality of the fit strongly depends on the charming penguins, since in this scenario one needs hadronic contributions to reproduce the angular distributions and BRs.

More general scenarios with two or more nonvanishing NP Wilson coefficients, such as scenario D, where C_{2223}^{LQ} and C_{2322}^{Qe} are allowed to float, or scenario E, where all the coefficients of the operators in eq. (3.1) are turned on, are slightly penalized by the number

	Approach	R_K [1.1, 6]	R_{K^*} [0.045, 1.1]	R_{K^*} [1.1, 6]	P'_5 [4, 6]	P'_5 [6, 8]	$B_s \to \mu\mu$ $\times 10^9$
Exp.	-	0.848(42)	0.680(93)	0.71(10)	-0.439(117)	-0.583(095)	2.86(33)
A	Data Driven	0.84(4)	0.86(4)	0.81(13)	-0.47(5)	-0.53(7)	3.58(11)
	LCSR $q^2 \leq 1$	0.76(4)	0.89(1)	0.85(3)	-0.44(5)	-0.55(6)	3.58(11)
	LCSR	0.76(2)	0.89(1)	0.83(1)	-0.45(4)	-0.59(4)	3.58(11)
B	Data Driven	0.83(4)	0.85(2)	0.75(5)	-0.48(5)	-0.54(7)	2.64(21)
	LCSR $q^2 \leq 1$	0.76(3)	0.86(1)	0.76(3)	-0.46(5)	-0.56(6)	2.74(11)
	LCSR	0.72(3)	0.85(1)	0.74(3)	-0.63(3)	-0.74(2)	2.65(10)
C	Data Driven	0.82(3)	0.86(1)	0.75(5)	-0.49(5)	-0.55(7)	2.56(19)
	LCSR $q^2 \leq 1$	0.83(2)	0.85(1)	0.76(3)	-0.48(5)	-0.57(6)	2.40(16)
	LCSR	0.84(3)	0.87(1)	0.74(3)	-0.73(3)	-0.80(2)	2.55(16)
D	Data Driven	0.83(4)	0.85(2)	0.75(6)	-0.49(5)	-0.55(7)	2.58(23)
	LCSR $q^2 \leq 1$	0.77(4)	0.85(1)	0.76(3)	-0.47(5)	-0.57(6)	2.67(21)
	LCSR	0.71(3)	0.87(1)	0.77(3)	-0.48(4)	-0.62(4)	3.20(16)
E	Data Driven	0.84(4)	0.82(4)	0.68(8)	-0.48(6)	-0.55(7)	2.54(29)
	LCSR $q^2 \leq 1$	0.79(4)	0.81(3)	0.65(8)	-0.47(5)	-0.56(6)	2.64(24)
	LCSR	0.80(4)	0.82(2)	0.67(4)	-0.49(4)	-0.64(4)	2.80(22)

Table 3. Experimental measurements with symmetrized errors (for R_{K^*} and P'_5 we report the LHCb ones) and posteriors for key observables in the SMEFT scenarios considered here. Scenario A corresponds to NP contributions to C_9 only; scenario B to NP contributions to C_{2223}^{LQ} only; scenario C to NP contributions to C_{10} only; scenario D to NP contributions to C_{2223}^{LQ} and C_{2322}^{Qe}; and scenario E to NP contributions to $C_{2223}^{LQ}, C_{2322}^{Qe}, C_{2223}^{Ld}$ and C_{2223}^{ed}.

of degrees of freedom unless the *fully model-dependent* hypothesis is considered, as can be seen from Table 2. For the reader's convenience, in Table 2 and in Figs. 5-7 we present results for scenarios D and E also in the weak effective Hamiltonian basis through eq. (3.2).

It is interesting to look at the shape of the probability density contours for the NP parameters in scenario D reported in Fig. 5. In the *fully data-driven* approach, $C_9^{\rm NP}$ is well compatible with 0, while a nonvanishing NP axial lepton coupling emerges from the experimental information coming from "clean observables". A slight preference for a nonvanishing $C_9^{\rm NP}$ is present in the *partly model-dependent* approach, while a strong evidence for $C_9^{\rm NP}$ is obtained in the *fully model-dependent* hypothesis, together with a slight hint of a nonvanishing $C_{10}^{\rm NP}$. Therefore, Fig. 5 represents a clear example of how the size of charming penguins can strongly impact the inference of the underlying NP picture, allowing to go from a purely axial NP coupling to a purely vectorial one in the two extreme cases, with dramatic consequences for the model building related to B anomalies.

Concerning scenario E, it is worth noticing that in the *fully model-dependent* approach right-handed operators allow to improve the agreement with R_K, given the current exper-
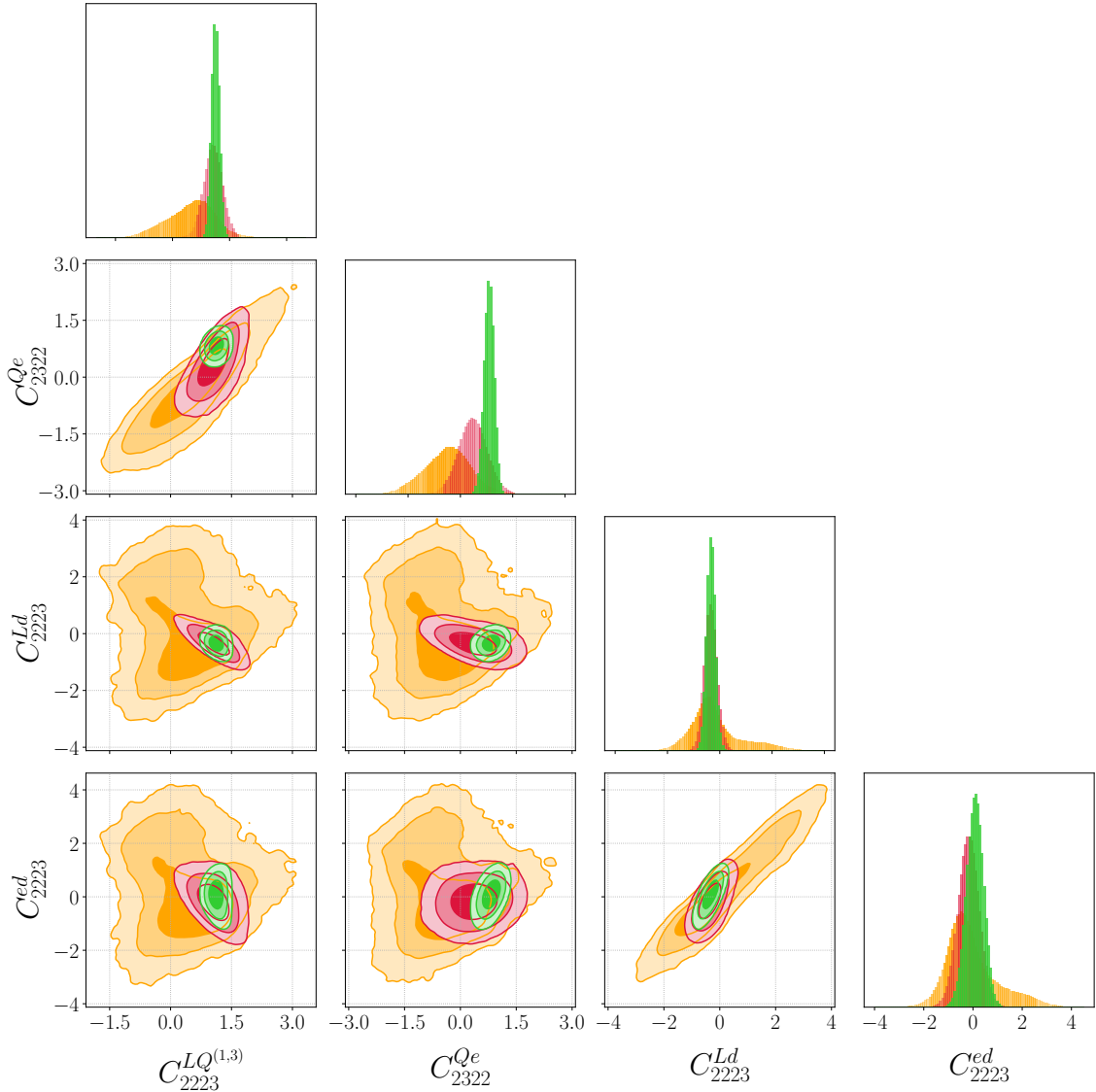
Figure 6. Posteriors for C^{LQ}_{2223}, C^{Qe}_{2322}, C^{Ld}_{2223} and C^{ed}_{2223}. Contours and colours as in Fig. 5.

imental hint for $R_K \neq R_{K^*}$ at the 1σ level, see the discussion in [59]. In the *fully data driven* and *partly model-dependent* cases this can be achieved also through the interplay of hadronic corrections with LUV NP (see Table 3). See Figs. 6 and 7 for a comparison of the posteriors for NP coefficients in scenario E.

4 Conclusions

We have presented a global analysis of the experimental data on $b \to s\ell^+\ell^-$ transitions from refs. [1–18] under three different assumptions about the size and shape of the charming penguin contribution: a *fully data driven* approach, a *partly model-dependent* and a *fully model-dependent* one. We have shown how current data point to a nontrivial helicity and
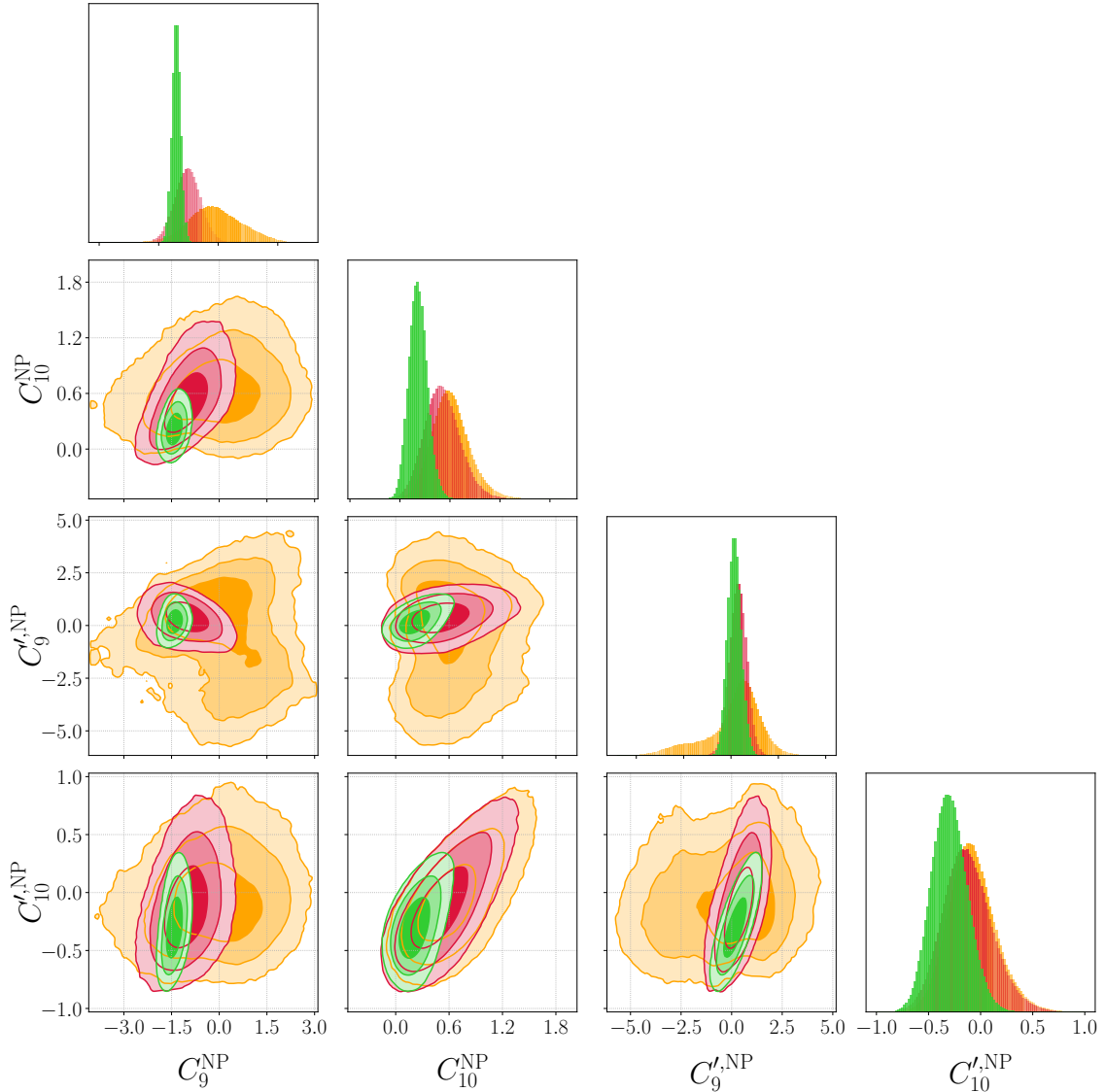
Figure 7. Posteriors for $C_9^{\mathrm{NP}}, C_{10}^{\mathrm{NP}}, C_9^{\prime,\mathrm{NP}}$ and $C_{10}^{\prime,\mathrm{NP}}$. Contours and colours as in Fig. 5.

q^2 dependence of the charm loop, although with no firm evidence so far. We have discussed the interplay of NP and hadronic contributions and the dependence of the inferred NP from the assumptions on the charm loop.

More conservative hypotheses point to two simple NP scenarios, either a nonvanishing C_{2223}^{LQ}, with a ΔIC with respect to the SM of 33 (53) in the *fully data driven* (*partly model-dependent*) approach, or a nonvanishing C_{10}^{NP}, with a ΔIC with respect to the SM of 34 (48) in the *fully data driven* (*partly model-dependent*) case. The *fully model-dependent* assumption, instead, favours a more complex scenario with four nonvanishing NP coefficients with a ΔIC of 98, although a ΔIC of 88 can be achieved in the simple scenario of a nonvanishing C_9^{NP}. Clearly, more data on both LUV observables and differential decay rates is needed to improve our understanding of the charm loop and to single out the cor-

rect interpretation of LUV in terms of NP contributions. Hopefully, the LHC [81, 82] and Belle II [83] will provide us with the needed precision to identify the NP at the origin of the current evidence of LUV.

Acknowledgments

References

[1] LHCB Collaboration, R. Aaij et al., *Test of lepton universality in beauty-quark decays*, arXiv:2103.11769.

[2] LHCB Collaboration, R. Aaij et al., *Tests of lepton universality using $B^0 \to K_S^0 l^+ l^-$ and $B^+ \to K^{*+}\ell^+\ell^-$ decays*, arXiv:2110.09501.

[3] LHCB Collaboration, R. Aaij et al., *Test of lepton universality with $B^0 \to K^{*0}\ell^+\ell^-$ decays*, *JHEP* **08** (2017) 055, [arXiv:1705.05802].

[4] BELLE Collaboration, A. Abdesselam et al., *Test of lepton flavor universality in $B \to K^*\ell^+\ell^-$ decays at Belle*, arXiv:1904.02440.

[5] CMS, LHCB Collaboration, V. Khachatryan et al., *Observation of the rare $B_s^0 \to \mu^+\mu^-$ decay from the combined analysis of CMS and LHCb data*, *Nature* **522** (2015) 68–72, [arXiv:1411.4413].

[6] LHCB Collaboration, R. Aaij et al., *Measurement of the $B_s^0 \to \mu^+\mu^-$ branching fraction and effective lifetime and search for $B^0 \to \mu^+\mu^-$ decays*, *Phys. Rev. Lett.* **118** (2017) 191801, [arXiv:1703.05747].

[7] ATLAS Collaboration, M. Aaboud et al., *Study of the rare decays of B_s^0 and B^0 mesons into muon pairs using data collected during 2015 and 2016 with the ATLAS detector*, *JHEP* **04** (2019) 098, [arXiv:1812.03017].

[8] CMS Collaboration, A. M. Sirunyan et al., *Measurement of properties of $B_s^0 \to \mu^+\mu^-$ decays and search for $B^0 \to \mu^+\mu^-$ with the CMS experiment*, *JHEP* **04** (2020) 188, [arXiv:1910.12127].

[9] LHCB Collaboration, R. Aaij et al., *Analysis of neutral B-meson decays into two muons*, arXiv:2108.09284.

[10] LHCB Collaboration, R. Aaij et al., *Angular analysis of the $B^+ \to K^{*+}\mu^+\mu^-$ decay*, arXiv:2012.13241.

[11] LHCв Collaboration, R. Aaij et al., *Measurement of CP-Averaged Observables in the $B^0 \to K^{*0}\mu^+\mu^-$ Decay*, *Phys. Rev. Lett.* **125** (2020) 011802, [arXiv:2003.04831].

[12] LHCв Collaboration, R. Aaij et al., *Angular analysis of the $B^0 \to K^{*0}\mu^+\mu^-$ decay using 3 fb^{-1} of integrated luminosity*, *JHEP* **02** (2016) 104, [arXiv:1512.04442].

[13] LHCв Collaboration, R. Aaij et al., *Differential branching fraction and angular analysis of the decay $B_s^0 \to \phi\mu^+\mu^-$*, *JHEP* **07** (2013) 084, [arXiv:1305.2168].

[14] LHCв Collaboration, R. Aaij et al., *Angular analysis and differential branching fraction of the decay $B_s^0 \to \phi\mu^+\mu^-$*, *JHEP* **09** (2015) 179, [arXiv:1506.08777].

[15] LHCв Collaboration, R. Aaij et al., *Branching Fraction Measurements of the Rare $B_s^0 \to \phi\mu^+\mu^-$ and $B_s^0 \to f_2'(1525)\mu^+\mu^-$- Decays*, *Phys. Rev. Lett.* **127** (2021) 151801, [arXiv:2105.14007].

[16] LHCв Collaboration, R. Aaij et al., *Angular analysis of the rare decay $B_s^0 \to \phi\mu^+\mu^-$*, arXiv:2107.13428.

[17] BELLE Collaboration, S. Wehle et al., *Lepton-Flavor-Dependent Angular Analysis of $B \to K^*\ell^+\ell^-$*, *Phys. Rev. Lett.* **118** (2017) 111801, [arXiv:1612.05014].

[18] BELLE Collaboration, A. Abdesselam et al., *Test of Lepton-Flavor Universality in $B \to K^*\ell^+\ell^-$ Decays at Belle*, *Phys. Rev. Lett.* **126** (2021) 161801, [arXiv:1904.02440].

[19] M. Bordone, G. Isidori and A. Pattori, *On the Standard Model predictions for R_K and R_{K^*}*, *Eur. Phys. J. C* **76** (2016) 440, [arXiv:1605.07633].

[20] G. Isidori, S. Nabeebaccus and R. Zwicky, *QED Corrections in $\bar{B} \to \bar{K}\ell^+\ell^-$ at the Double-Differential Level*, arXiv:2009.00929.

[21] M. Ciuchini, E. Franco, G. Martinelli and L. Silvestrini, *Charming penguins in B decays*, *Nucl. Phys. B* **501** (1997) 271–296, [arXiv:hep-ph/9703353].

[22] M. Ciuchini, R. Contino, E. Franco, G. Martinelli and L. Silvestrini, *Charming penguin enhanced B decays*, *Nucl. Phys. B* **512** (1998) 3–18, [arXiv:hep-ph/9708222].

[23] M. Ciuchini, E. Franco, G. Martinelli, M. Pierini and L. Silvestrini, *Charming penguins strike back*, *Phys. Lett. B* **515** (2001) 33–41, [arXiv:hep-ph/0104126].

[24] M. Beneke, G. Buchalla, M. Neubert and C. T. Sachrajda, *QCD factorization for $B \to \pi\pi$ decays: Strong phases and CP violation in the heavy quark limit*, *Phys. Rev. Lett.* **83** (1999) 1914–1917, [arXiv:hep-ph/9905312].

[25] M. Beneke, G. Buchalla, M. Neubert and C. T. Sachrajda, *QCD factorization for exclusive, nonleptonic B meson decays: General arguments and the case of heavy light final states*, *Nucl. Phys.* **B591** (2000) 313–418, [arXiv:hep-ph/0006124].

[26] M. Beneke, T. Feldmann and D. Seidel, *Exclusive radiative and electroweak $b \to d$ and $b \to s$ penguin decays at NLO*, *Eur. Phys. J. C* **41** (2005) 173–188, [arXiv:hep-ph/0412400].

[27] S. Descotes-Genon, T. Hurth, J. Matias and J. Virto, *Optimizing the basis of $B \to K^*ll$ observables in the full kinematic range*, *JHEP* **05** (2013) 137, [arXiv:1303.5794].

[28] S. Descotes-Genon, L. Hofer, J. Matias and J. Virto, *On the impact of power corrections in the prediction of $B \to K^*\mu^+\mu^-$ observables*, *JHEP* **12** (2014) 125, [arXiv:1407.8526].

[29] S. Jäger and J. Martin Camalich, *On $B \to V\ell\ell$ at small dilepton invariant mass, power corrections, and new physics*, *JHEP* **05** (2013) 043, [arXiv:1212.2263].

[30] S. Jäger and J. Martin Camalich, *Reassessing the discovery potential of the $B \to K^*\ell^+\ell^-$ decays in the large-recoil region: SM challenges and BSM opportunities*, *Phys. Rev. D* **93** (2016) 014028, [arXiv:1412.3183].

[31] M. Ciuchini, M. Fedele, E. Franco, S. Mishima, A. Paul, L. Silvestrini et al., *$B \to K^*\ell^+\ell^-$ decays at large recoil in the Standard Model: a theoretical reappraisal*, *JHEP* **06** (2016) 116, [arXiv:1512.07157].

[32] M. Ciuchini, M. Fedele, E. Franco, S. Mishima, A. Paul, L. Silvestrini et al., *$B \to K^*\ell^+\ell^-$ in the Standard Model: Elaborations and Interpretations*, *PoS* **ICHEP2016** (2016) 584, [arXiv:1611.04338].

[33] A. Arbey, T. Hurth, F. Mahmoudi and S. Neshatpour, *Hadronic and New Physics Contributions to $b \to s$ Transitions*, *Phys. Rev. D* **98** (2018) 095027, [arXiv:1806.02791].

[34] M. Ciuchini, A. M. Coutinho, M. Fedele, E. Franco, A. Paul, L. Silvestrini et al., *Hadronic uncertainties in semileptonic $B \to K^*\mu^+\mu^-$ decays*, *PoS* **BEAUTY2018** (2018) 044, [arXiv:1809.03789].

[35] T. Hurth, F. Mahmoudi and S. Neshatpour, *Implications of the new LHCb angular analysis of $B \to K^*\mu^+\mu^-$: Hadronic effects or new physics?*, *Phys. Rev. D* **102** (2020) 055001, [arXiv:2006.04213].

[36] M. Beneke, G. Buchalla, M. Neubert and C. Sachrajda, *Penguins with Charm and Quark-Hadron Duality*, *Eur. Phys. J. C* **61** (2009) 439–449, [arXiv:0902.4446].

[37] C. Bobeth, M. Chrzaszcz, D. van Dyk and J. Virto, *Long-distance effects in $B \to K^*\ell\ell$ from analyticity*, *Eur. Phys. J. C* **78** (2018) 451, [arXiv:1707.07305].

[38] D. Melikhov, *Charming loops in exclusive rare FCNC B-decays*, *EPJ Web Conf.* **222** (2019) 01007, [arXiv:1911.03899].

[39] G. Hiller and F. Kruger, *More model-independent analysis of $b \to s$ processes*, *Phys. Rev. D* **69** (2004) 074020, [arXiv:hep-ph/0310219].

[40] C. Bobeth, G. Hiller and G. Piranishvili, *Angular distributions of $\bar{B} \to \bar{K}\ell^+\ell^-$ decays*, *JHEP* **12** (2007) 040, [arXiv:0709.4174].

[41] G. Hiller, D. Loose and I. Nišandžić, *Flavorful leptoquarks at the LHC and beyond: spin 1*, *JHEP* **06** (2021) 080, [arXiv:2103.12724].

[42] L.-S. Geng, B. Grinstein, S. Jäger, S.-Y. Li, J. Martin Camalich and R.-X. Shi, *Implications of new evidence for lepton-universality violation in $b \to s\ell^+\ell^-$ decays*, *Phys. Rev. D* **104** (2021) 035029, [arXiv:2103.12738].

[43] C. Cornella, D. A. Faroughy, J. Fuentes-Martin, G. Isidori and M. Neubert, *Reading the footprints of the B-meson flavor anomalies*, *JHEP* **08** (2021) 050, [arXiv:2103.16558].

[44] T. Hurth, F. Mahmoudi, D. M. Santos and S. Neshatpour, *More Indications for Lepton Nonuniversality in $b \to s\ell^+\ell^-$*, arXiv:2104.10058.

[45] M. Algueró, B. Capdevila, S. Descotes-Genon, J. Matias and M. Novoa-Brunet, *$b \to s\ell\ell$ global fits after Moriond 2021 results*, in *55th Rencontres de Moriond on QCD and High Energy Interactions*, 4, 2021. arXiv:2104.08921.

[46] R. Bause, H. Gisbert, M. Golz and G. Hiller, *Interplay of dineutrino modes with semileptonic rare B-decays*, arXiv:2109.01675.

[47] A. Crivellin, C. A. Manzari, M. Alguero and J. Matias, *Combined Explanation of the $Z \to b\bar{b}$ Forward-Backward Asymmetry, the Cabibbo Angle Anomaly, $\tau \to \mu\nu\nu$ and $b \to s\ell^+\ell^-$ Data*, arXiv:2010.14504.

[48] A. Crivellin, M. Hoferichter and C. A. Manzari, *Fermi Constant from Muon Decay Versus Electroweak Fits and Cabibbo-Kobayashi-Maskawa Unitarity*, *Phys. Rev. Lett.* **127** (2021) 071801, [arXiv:2102.02825].

[49] A. Crivellin, C. A. Manzari and M. Montull, *Correlating Non-Resonant Di-Electron Searches at the LHC to the Cabibbo-Angle Anomaly and Lepton Flavour Universality Violation*, arXiv:2103.12003.

[50] P. Arnan, A. Crivellin, M. Fedele and F. Mescia, *Generic Loop Effects of New Scalars and Fermions in $b \to s\ell^+\ell^-$, $(g-2)_\mu$ and a Vector-like 4th Generation*, *JHEP* **06** (2019) 118, [arXiv:1904.05890].

[51] A. Datta, J. L. Feng, S. Kamali and J. Kumar, *Resolving the $(g-2)_\mu$ and B Anomalies with Leptoquarks and a Dark Higgs Boson*, *Phys. Rev. D* **101** (2020) 035010, [arXiv:1908.08625].

[52] A. Greljo, P. Stangl and A. E. Thomsen, *A model of muon anomalies*, *Phys. Lett. B* **820** (2021) 136554, [arXiv:2103.13991].

[53] G. Arcadi, L. Calibbi, M. Fedele and F. Mescia, *Muon $g-2$ and B-anomalies from Dark Matter*, *Phys. Rev. Lett.* **127** (2021) 061802, [arXiv:2104.03228].

[54] D. Marzocca and S. Trifinopoulos, *Minimal Explanation of Flavor Anomalies: B-Meson Decays, Muon Magnetic Moment, and the Cabibbo Angle*, *Phys. Rev. Lett.* **127** (2021) 061803, [arXiv:2104.05730].

[55] P. F. Perez, C. Murgui and A. D. Plascencia, *Leptoquarks and matter unification: Flavor anomalies and the muon g-2*, *Phys. Rev. D* **104** (2021) 035041, [arXiv:2104.11229].

[56] L. Darmé, M. Fedele, K. Kowalska and E. M. Sessolo, *Flavour anomalies and the muon $g-2$ from feebly interacting particles*, arXiv:2106.12582.

[57] A. Greljo, Y. Soreq, P. Stangl, A. E. Thomsen and J. Zupan, *Muonic Force Behind Flavor Anomalies*, arXiv:2107.07518.

[58] M. Ciuchini, A. M. Coutinho, M. Fedele, E. Franco, A. Paul, L. Silvestrini et al., *On Flavourful Easter eggs for New Physics hunger and Lepton Flavour Universality violation*, *Eur. Phys. J.* **C77** (2017) 688, [arXiv:1704.05447].

[59] M. Ciuchini, A. M. Coutinho, M. Fedele, E. Franco, A. Paul, L. Silvestrini et al., *New Physics in $b \to s\ell^+\ell^-$ confronts new data on Lepton Universality*, *Eur. Phys. J. C* **79** (2019) 719, [arXiv:1903.09632].

[60] M. Ciuchini, M. Fedele, E. Franco, A. Paul, L. Silvestrini and M. Valli, *Lessons from the $B^{0,+} \to K^{*0,+}\mu^+\mu^-$ angular analyses*, *Phys. Rev. D* **103** (2021) 015030, [arXiv:2011.01212].

[61] G. Isidori, D. Lancierini, P. Owen and N. Serra, *On the significance of new physics in $b \to s\ell^+\ell^-$ decays*, *Phys. Lett. B* **822** (2021) 136644, [arXiv:2104.05631].

[62] J. Gratrex, M. Hopfer and R. Zwicky, *Generalised helicity formalism, higher moments and the $B \to K_{J_K}(\to K\pi)\bar{\ell}_1\ell_2$ angular distributions*, *Phys. Rev.* **D93** (2016) 054008, [arXiv:1506.03970].

[63] A. Bharucha, D. M. Straub and R. Zwicky, *$B \to V\ell^+\ell^-$ in the Standard Model from light-cone sum rules*, *JHEP* **08** (2016) 098, [arXiv:1503.05534].

[64] N. Gubernari, A. Kokulu and D. van Dyk, *B → P and B → V Form Factors from B-Meson Light-Cone Sum Rules beyond Leading Twist*, *JHEP* **01** (2019) 150, [arXiv:1811.00983].

[65] V. G. Chobanova, T. Hurth, F. Mahmoudi, D. Martinez Santos and S. Neshatpour, *Large hadronic power corrections or new physics in the rare decay B → K*μ+μ− ?*, *JHEP* **07** (2017) 025, [arXiv:1702.02234].

[66] L. Maiani and M. Testa, *Final state interactions from Euclidean correlation functions*, *Phys. Lett. B* **245** (1990) 585–590.

[67] A. Khodjamirian, T. Mannel, A. Pivovarov and Y.-M. Wang, *Charm-loop effect in B → K(*)ℓ+ℓ− and B → K*γ*, *JHEP* **09** (2010) 089, [arXiv:1006.4945].

[68] N. Gubernari, D. van Dyk and J. Virto, *Non-local matrix elements in B(s) → {K(*), φ}ℓ+ℓ−*, *JHEP* **02** (2021) 088, [arXiv:2011.09813].

[69] S. Descotes-Genon, J. Matias, M. Ramon and J. Virto, *Implications from clean observables for the binned analysis of B− > K ∗ μ+μ− at large recoil*, *JHEP* **01** (2013) 048, [arXiv:1207.2753].

[70] J. De Blas et al., *HEPfit: a code for the combination of indirect and direct constraints on high energy physics models*, *Eur. Phys. J. C* **80** (2020) 456, [arXiv:1910.14012].

[71] "HEPfit: a tool to combine indirect and direct constraints on High Energy Physics." http://hepfit.roma1.infn.it/.

[72] T. Blake, U. Egede, P. Owen, K. A. Petridis and G. Pomery, *An empirical model to determine the hadronic resonance contributions to B̄0 → K̄*0μ+μ− transitions*, *Eur. Phys. J. C* **78** (2018) 453, [arXiv:1709.03921].

[73] M. Chrzaszcz, A. Mauri, N. Serra, R. Silva Coutinho and D. van Dyk, *Prospects for disentangling long- and short-distance effects in the decays B → K*μ+μ−*, *JHEP* **10** (2019) 236, [arXiv:1805.06378].

[74] A. Celis, J. Fuentes-Martin, A. Vicente and J. Virto, *Gauge-invariant implications of the LHCb measurements on lepton-flavor nonuniversality*, *Phys. Rev. D* **96** (2017) 035026, [arXiv:1704.05672].

[75] L. Alasfar, A. Azatov, J. de Blas, A. Paul and M. Valli, *B anomalies under the lens of electroweak precision*, *JHEP* **12** (2020) 016, [arXiv:2007.04400].

[76] S. Jäger, M. Kirk, A. Lenz and K. Leslie, *Charming new physics in rare B-decays and mixing?*, *Phys. Rev. D* **97** (2018) 015021, [arXiv:1701.09183].

[77] S. Jäger, M. Kirk, A. Lenz and K. Leslie, *Charming New B-Physics*, *JHEP* **03** (2020) 122, [arXiv:1910.12924].

[78] J. Aebischer, A. Crivellin, M. Fael and C. Greub, *Matching of gauge invariant dimension-six operators for b → s and b → c transitions*, *JHEP* **05** (2016) 037, [arXiv:1512.02830].

[79] T. Ando, *Predictive bayesian model selection*, *American Journal of Mathematical and Management Sciences* **31** (2011) 13–38.

[80] R. E. Kass and A. E. Raftery, *Bayes factors*, *Journal of the American Statistical Association* **90** (1995) 773–795.

[81] A. Cerri et al., *Report from Working Group 4: Opportunities in Flavour Physics at the HL-LHC and HE-LHC*, *CERN Yellow Rep. Monogr.* **7** (2019) 867–1158, [arXiv:1812.07638].

[82] LHCB COLLABORATION Collaboration, R. Aaij et al., *Expression of Interest for a Phase-II LHCb Upgrade: Opportunities in flavour physics, and beyond, in the HL-LHC era*, Tech. Rep. CERN-LHCC-2017-003, CERN, Geneva, Feb, 2017.

[83] BELLE-II Collaboration, W. Altmannshofer et al., *The Belle II Physics Book*, *PTEP* **2019** (2019) 123C01, [arXiv:1808.10567].